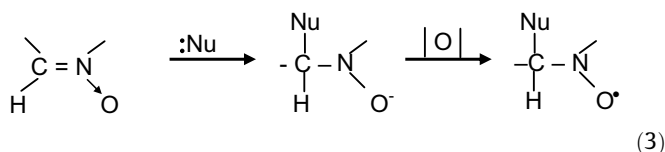


Fig. 1. Chemical structures of DMPO, POBN, PBN, and their oxidized forms.



The aim of the present work was to characterize the products of the reaction between Tl(III) and nitrones in aqueous solutions and the mechanisms involved in the process, which, to our best knowledge were not investigated until now. Diverse metal cations have been demonstrated to react with nitrones but the mechanism involved is not unique, and even the contribution of oxygen free radicals is not a common rule. As a consequence, the reaction between this metal and nitrones deserves to be analyzed not only for the merely chemical point of view interest, but also for its significance in biological and pharmaceutical fields. Results indicate that Tl(III) caused the oxidation of DMPO with formation of DMPOX. This oxidation product was not formed through a simple ionic oxidation of the nitron, and hydroxyl radical or other reactive oxygen species were not involved in the process. Based on our experimental findings, we proposed a possible mechanism to account for the formation of DMPOX.

2. Experimental

2.1. Chemicals

Thallium(III) nitrate and thallium(I) nitrate were from Alfa Aesar (Ward Hill, MA, USA). 5,5-dimethyl-1-pyrroline N-oxide (DMPO), α -phenyl-*N*-tertbutylnitron (PBN), α -(4-pyridyl-1-oxide)-*N*-tertbutylnitron (POBN), catalase (CAT), superoxide dismutase (SOD), trifluoperazine dihydrochloride (TFP), α -hydroxyisobutyric acid (HIBA) and 18-Crown-6-ether were obtained from Sigma-Aldrich (St. Louis, MO, USA). Imidazole and glacial acetic acid were supplied by E. Merck (Darmstadt, Germany). Ethanol, methanol, mannitol, Tris-HCl, and HEPES were of analytical grade.

To improve its purity, DMPO solutions were treated with activated charcoal. The DMPO concentration was measured at 232 nm, assuming molar absorption coefficient of $7700 \text{ M}^{-1} \text{ cm}^{-1}$ [6]. Ultrapure (Milli Q) water was used to prepare all the solutions, except in capillary electrophoresis assays where the ultrapure water was obtained from an EASY pureTM RF equipment (Barnstead, Dubuque, IA, USA).

2.2. Tl solutions

Tl(III) stock solutions were prepared immediately before assays, dissolving Tl(III) nitrate in Milli Q water and acidified with 3 M HCl until the attainment of a colorless solution. The amount of acidic Tl(III) solution used for the experiments did not alter the pH of the buffer solutions used in the experiments. Tl(I) stock solutions were prepared in Milli Q water.

2.3. ESR measurements

ESR spectra were recorded at room temperature ($20 \pm 1 \text{ }^\circ\text{C}$) in a Bruker spectrometer ECS 106 (Karlsruhe, Germany) with an ER 4102ST cavity. Typical spectrometer settings were: field modulation frequency, 50 kHz; microwave frequency, 9.81 GHz; modulation amplitude, 0.5 G; microwave power, 20 mW; time constant, 655 ms; sweep width, 100 G; center field, 3480 G; number of scans, 1. Reactions were initiated by the addition of Tl(III) and the reaction mixture was immediately transferred to disposable glass Pasteur pipettes.

Quantification of the spin adducts was performed by using Tempol standard solutions.

2.4. Tl(III) and Tl(I) determination

Tl(III) concentration after incubation in the presence of DMPO was evaluated spectrophotometrically [7]. DMPO (10 mM) in Milli Q water was incubated at room temperature in the presence of Tl(III) (15–100 μM). At different time points, a 70 μl aliquot was transferred to a 96-well microplate containing 0.130 ml of TFP (0.73% final concentration) in 10 M phosphoric acid. Samples were incubated for 30 min at 37 $^\circ\text{C}$, and the absorbance at 492 nm was registered in a Biotrak II plate reader (Amersham Biosciences). The concentration of Tl(III) in the samples was calculated using a standard curve run in parallel.

Tl(I) was quantitatively determined by capillary electrophoresis (CE) with UV absorption at 214 nm. The background electrolyte was prepared by dissolving 6 mM imidazole, 10 mM HIBA and 1 mM 18-Crown-6-ether in water, and the solution was adjusted to pH 4.0 with glacial acetic acid. All solutions were filtered through a 0.45 μm nylon membrane (Micron Separations Inc., USA). The operating conditions were hydrostatic injection (10 cm height) for 30 s, applied voltage: +25 kV, and temperature set at 30 $^\circ\text{C}$. All CE separations were performed with a Capillary Ion Analyzer (Waters Corp., Milford, MA, USA) using uncoated fused-silica capillary of 60 cm length (53 cm to detector) and 75 μm I.D. (MicroSolv Technology Corp., Eatontown, NJ, USA). Data were processed by Empower Pro software (Waters).

2.5. Statistics

Statistical differences between two groups were evaluated by the Student's *t*-test using the computer software StatView 5.0 (SAS Institute Inc., Cary, NC, USA). A probability (*P*) value lower than 0.05 was considered to be statistically significant.

3. Results and discussion

3.1. DMPOX formation: the origin of the oxygen atom

In a system containing DMPO (10 mM) and Tl(III) (25 μM) in 20 mM Tris-HCl buffer (pH 7.4), a strong ESR signal was observed immediately after sample preparation at room temperature (Fig. 2). The spectrum was assigned to 5,5-dimethylpyrrolidone-2-(oxy)-(1) or 5,5-dimethyl-1-pyrrolidone-2-oxyl (DMPOX, Fig. 1)

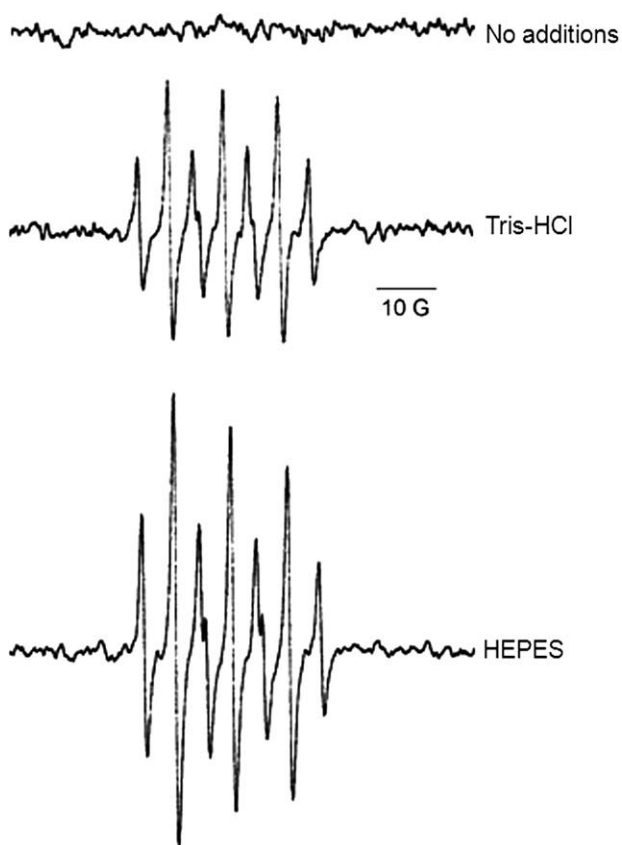


Fig. 2. First-derivative ESR spectra of DMPO-derived product. Aliquots of 20 mM Tris-HCl or 20 mM HEPES buffers (pH 7.4) containing 10 mM DMPO were incubated at room temperature in the presence of 25 μM Tl(III). After 2 min, ESR spectra were obtained as described in Section 2. Traces correspond to representative experiments ($n = 4$).

[8–11] from its hyperfine coupling constants ($a^{\text{N}}(1) = 7.3 \pm 0.1$ G and $a^{\text{H}}(2) = 3.9 \pm 0.1$ G). When the reaction was carried out in the presence of 20 mM HEPES (pH 7.4), signal intensity was 2-fold higher (Fig. 2), suggesting that the composition of the buffer solution determined the extent of the reaction. In fact, when the buffer contained strong metal ligands, such as phosphate or carboxylate, no DMPOX was detected (data not shown).

DMPOX is the main product in many diverse systems containing DMPO plus hematin-cumene hydroperoxide [9], *tert*-butylhydroperoxide and Ce(IV) [11], cytochrome *c* and H_2O_2 [12], Fe(III) or Cu(II) [13], ClO_2 [14], metallic Co in aqueous suspension [15], or Au(III) [16], and it also is a minor product in the reaction between cytochrome *c* or methemoglobin/metmyoglobin and organic hydroperoxides [17,18]. Different mechanisms have been proposed to explain the origin of the oxygen atom which adds to the 2-position of DMPO. In the present study there are two possible sources for this oxygen atom: dissolved O_2 and water.

In order to investigate the role of oxygen free radicals that could be generated from the reaction between Tl(III) and dissolved O_2 , samples were added with several free-radical scavengers (Table 1). Given that Tl(III) could oxidize O_2 either by one or two-electron reactions, superoxide anion ($\text{O}_2^{\cdot-}$) or hydrogen peroxide (H_2O_2) could be, respectively, generated. The presence of superoxide dismutase (SOD, 100 mU) or catalase (CAT, 100 mU), which enzymatically degrade $\text{O}_2^{\cdot-}$ and H_2O_2 , respectively, failed to prevent DMPOX generation. To assess whether hydroxyl radical could be generated as a possible by-product, the reaction was also performed in the presence of mannitol (50 mM) or ethanol (50%, v/v) that scavenge hydroxyl radical with high rate constants [19].

Table 1
Effect of free-radical scavengers on DMPOX production.

Condition	Relative amount
25 μM Tl(III) + 10 mM DMPO	100
+SOD (100 mU)	92 \pm 7
+CAT (100 mU)	85 \pm 9
+Mannitol (50 mM)	96 \pm 6
+Ethanol (50%, v/v)	78 \pm 10
+Methanol (50%, v/v)	111 \pm 17
+Methanol (90%, v/v)	18 \pm 6
+Methanol (99%, v/v)	ND

Results are expressed as the relative amount respect to the signal intensity obtained after the reaction at 15 $^\circ\text{C}$ between 25 μM Tl(III) and 10 mM DMPO in a 20 mM Tris-HCl buffer, pH 7.4. ND: non-detectable.

Under these conditions, the intensity of DMPOX signal was not affected. Supporting this, no effect on the reaction was observed when methanol, another hydroxyl radical scavenger [20] was added up to a 50% (v/v) final concentration (Table 1).

Further experimental evidence sustains the lack of hydroxyl radical participation in Tl(III)-mediated DMPOX formation. It has been extensively described that hydroxyl radical is able to subtract a hydrogen atom from either ethanol or methanol, resulting in the formation of α -hydroxyethyl radical ($\text{CH}_3\cdot\text{CH}_2\text{OH}$) and hydroxymethyl radical ($\cdot\text{CH}_2\text{OH}$), respectively. Both of them are efficiently trapped by DMPO yielding stable adducts with characteristic six-line spectra [21]. In our experimental conditions, we did not observe the presence of these adducts, supporting the idea of a free-radical-independent mechanism for Tl(III)-supported DMPO oxidation.

In order to study the role of water in DMPOX formation, the concentration of methanol was raised. The amount of DMPOX detected was 82% lower ($P < 0.01$) at a 90% (v/v) methanol concentration, while no detectable DMPOX signal was observed in 100% (v/v) methanol solution (Table 1). These results indicate that water is the limiting reagent, and support the hypothesis of the involvement of a water nucleophilic addition in the process.

3.2. Reaction with non-cyclic nitrones: POBN and PBN

For the above discussed results, Tl(III)-mediated DMPO oxidation could not be explained by the mechanism described in Eq. (1), and thus the next two mechanisms were evaluated. In order to proceed through an “inverted spin-trapping” mechanism, the spin trap must be initially oxidized to its radical ($\text{DMPO}^{\cdot+}$) via a one-electron reaction. To investigate this possibility, we extended the study using the non-cyclic nitrones POBN and PBN (Fig. 1), since inverted spin-trapping preferentially occurs with this kind of molecules, rather than with DMPO [16,22]. The resultant spectra did not show the signals corresponding to the oxidized species POBNX and PBNX [14] (Fig. 3, simulated spectra). Instead, POBN showed a weak but clear spectrum, a triplet ESR signal, with $a^{\text{N}}(1) = 16.6$ G and non-detectable splitting due to hydrogen atoms (Fig. 3) that did not correspond to POBNX. This signal was only observed when samples were incubated for 1 h at 37 $^\circ\text{C}$ in the presence of 100 μM Tl(III), and the amount of accumulated scans necessary to achieve a well-defined spectrum raised to six. Similarly to the observed for DMPO, in 20 mM HEPES buffer there was an increase in signal intensity. On the other hand no signal was detected for PBN neither in Tris-HCl nor in HEPES buffers.

The structure of PBN and POBN are similar, both having an aliphatic nitron group with an *N-tert*-butyl substituent and an aromatic ring bound to the α -carbon, and only differing in the nature of this aromatic ring: a benzene group and an *N*-oxide-pyridine group, respectively (Fig. 1). POBN has a second nitron moiety, the *N*-oxide-pyridine group, that is absent in PBN. Pyridine is

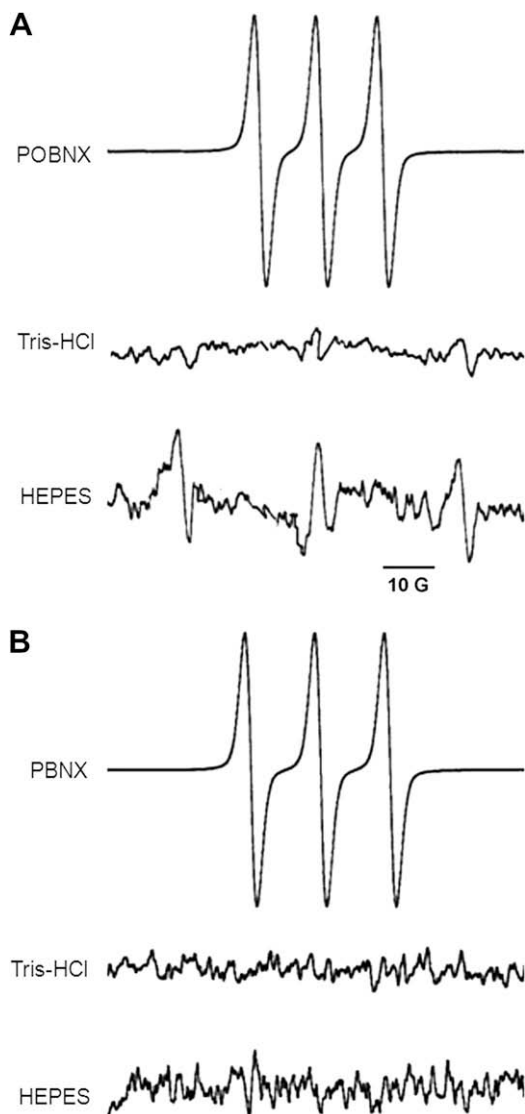


Fig. 3. First-derivative ESR spectra of POBN- and PBN-derived products. Aliquots of 20 mM Tris-HCl or 20 mM HEPES buffers (pH 7.4) containing either (A) 100 mM POBN, or (B) 50 mM PBN, were incubated in the absence or presence of 100 μ M Tl(III). Instrumental parameters were similar than the described in Section 2 (number of accumulated scans: 6). Traces indicated as POBNX and PBNX correspond to the simulated spectra using the following parameters: POBNX: line width, 2 G; line shape, 50% Lorentzian and 50% Gaussian; $a^N(1) = 7.6$ G; PBNX: line width, 2 G; line shape, 50% Lorentzian and 50% Gaussian; $a^N(1) = 8.5$ G. Traces correspond to representative experiments ($n = 3$).

susceptible to nucleophilic attacks, and this kind of reaction proceeds even faster on its N-oxide derivate. The lack of PBN adducts production and the presence of a signal with POBN would imply

that the aliphatic nitronne unit is not involved in the process, but rather it would be the pyridyl-associated nitronne moiety. Participation of this second nitronne group in the POBN-adducts formation is not usually considered, but it has been postulated as a possible route in the peroxidase-mediated oxidation of desferoxamine [23].

3.3. Forrester–Hepburn as a proposed mechanism

Taking into account these results, we propose that Tl(III) complexation with DMPO facilitated the water nucleophilic attack to the 2-position of DMPO ring (Fig. 4). As a consequence, DMPO-OH is formed in an equilibrium process [5,13], followed by a Tl(III)-mediated oxidation to a keto group. The first part of this process can be included in the reduced group of reactions that proceed through a Forrester–Hepburn mechanism [24]. The initial step is similar to that described for DMPO reaction with Fe(III) and Cu(II) yielding DMPO-OH [13]. However, and opposite to the mechanism described for these cations [13], DMPO-OH is not the final product when Tl(III) is the involved metal. In a second step, a two-electron oxidation renders DMPOX and Tl(I). Tl(III) has demonstrated to be an oxidant for secondary alcohols [25,26], like the OH group present in the DMPO-OH. The high oxidation potential of Tl(III)/Tl(I) (+1.25 V) [4] would be responsible for this redox reaction, while Fe(III) (+0.771 V) or Cu(II) (+0.167 V) [27] are not able to produce DMPOX.

To further characterize the mechanism of reaction, the effect of a strong nucleophile on DMPOX formation was assayed replacing water with 2 M methoxide in methanol. Reaction mixture showed a six-line spectrum assigned to DMPO-OCH₃ based on its hyperfine splitting constants ($a^N(1) = 13.7 \pm 0.1$ G and $a^H(1) = 8.1 \pm 0.2$ G) [28,29] (data not shown). Tl(III) increased DMPO-OCH₃ formation (5.5-fold increase) supporting the hypothesis of an inductive role of Tl(III) in methoxide nucleophilic addition. The oxidation step did not proceed due to the presence of the methyl substituent that impeded the final formation of DMPOX.

3.4. Kinetic analysis of DMPOX generation

The kinetics of DMPOX formation was followed by ESR in mixtures of a fixed DMPO initial concentration ($[DMPO]_0 = 10$ mM) and different Tl(III) initial concentrations ($[Tl(III)]_0 = 7.5$ – 10 μ M). Under our experimental conditions, radical concentration increased linearly during the first 5 min (data not shown), and DMPOX formation was calculated from the slope of the curves, obtaining $(1.05 \pm 0.05) \times 10^{-2}$ and $(1.75 \pm 0.03) \times 10^{-2}$ μ M s⁻¹ for 7.5 and 10 μ M $[Tl(III)]_0$, respectively.

On the other hand, time course of Tl(III) disappearance was determined by a spectrophotometric method that required the use of higher Tl(III) initial concentrations ($[Tl(III)]_0 = 25$ – 100 μ M) at the same fixed DMPO initial concentration ($[DMPO]_0 = 10$ mM). Initial rates (v_0 , $Tl(III)$) were calculated for each condition, and the plot of v_0 against $[Tl(III)]_0$ adjusted to a straight line that passed through the origin, indicating an unit order ($\beta = 1$) respect to the

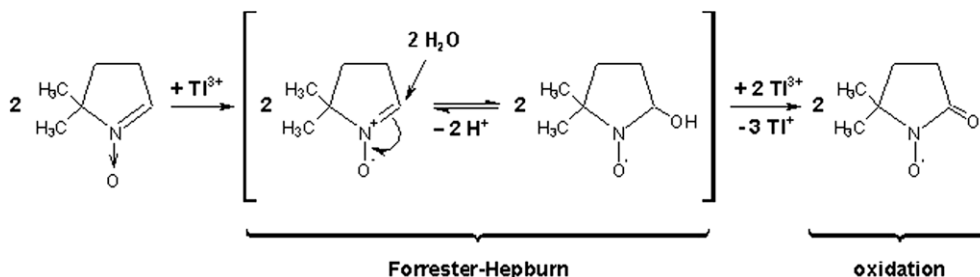


Fig. 4. Mechanism proposed for Tl(III)-mediated DMPOX formation. For details, see text.

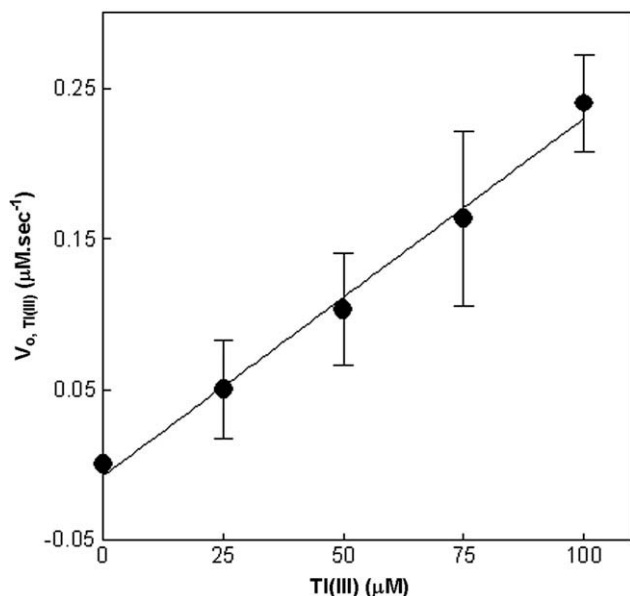


Fig. 5. Dependence of Tl(III) consumption initial rate ($v_{0, \text{Tl(III)}}$) on Tl(III) concentration. Kinetics of Tl(III) consumption was studied spectrophotometrically in reaction mixtures containing 10 mM DMPO in 20 mM Tris–HCl buffer (pH 7.4), and Tl(III) (25–100 μM). Results are shown as the mean \pm SEM ($n = 4$).

oxidant (Fig. 5). According to Eq. (4), the pseudo-first order constant (k') was $2.5 \times 10^{-3} \text{ s}^{-1}$

$$v_{0, \text{Tl(III)}} = -\frac{d[\text{Tl(III)}]}{dt} = k[\text{DMPO}]_0^{\alpha} [\text{Tl(III)}]_0^{\beta} = k' [\text{Tl(III)}]_0^{\beta} \quad (4)$$

In order to compare Tl(III) consumption rates with the experimental values obtained for DMPOX formation, rates calculated from Eq. (4) were $1.88 \times 10^{-2} \mu\text{M s}^{-1}$ and $2.52 \times 10^{-2} \mu\text{M s}^{-1}$ for 7.5 and 10 μM Tl(III), respectively. Taking in account these values, it is possible to

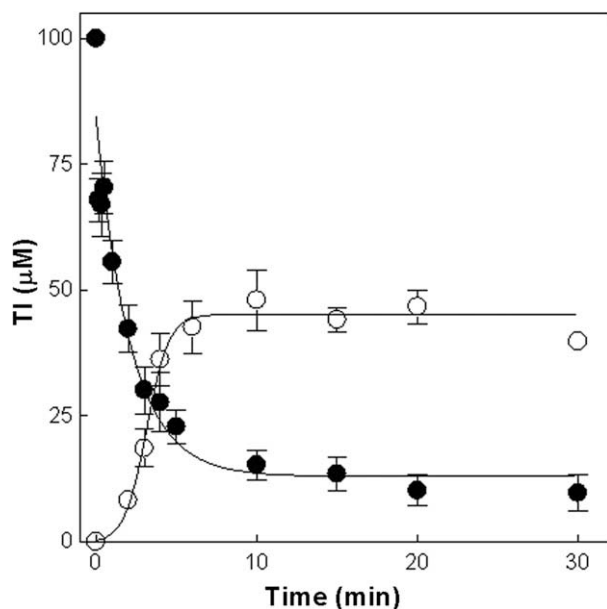


Fig. 6. Time course of the changes in Tl(III) (●) and Tl(I) (○) concentration along the reaction. Reaction mixtures contained 10 mM DMPO in Milli-Q water and 100 μM Tl(III) initial concentration. Tl(III) and Tl(I) concentrations in the mixture were quantitated spectrophotometrically and by capillary electrophoresis, respectively, and as described in Section 2. Results are shown as the mean \pm SEM ($n = 3$).

conclude that the rate of Tl(III) consumption was, in average, 1.6-times higher than the rate of DMPOX formation. This result shows that more than one Tl(III) ion (~ 1.5 ions) are involved in the formation of one DMPOX molecule, suggesting a 1.5:1 stoichiometry for Tl(III):DMPO reaction.

Tl oxidation state at the end of the reaction and its production rate were next investigated. By using CE it was possible to specifically detect Tl(I) as the final product, and to quantify the amount of Tl(I) produced along the reaction. Fig. 6 shows the time course of the variation of both Tl ionic species concentration when the reaction was carried out in Milli Q water and in the presence of 100 μM Tl(III) and 10 mM DMPO. These conditions were selected to be the most sensitive for CE determinations.

The rate of Tl(III) disappearance ($0.24 \pm 0.03 \mu\text{M s}^{-1}$) and the rate of Tl(I) formation ($0.23 \pm 0.04 \mu\text{M s}^{-1}$) resulted identical, suggesting a 1:1 stoichiometry in the global reaction. Surprisingly, at the equilibrium, the sum of the two ionic species was not 100 μM . The difference could be ascribed to a fraction of Tl(I) that remained complexed to DMPO and/or its reaction products in a way that becomes non-detectable for the CE system here implemented.

3.5. Effect of the pH on DMPOX formation

Finally, the dependence of Tl(III)-mediated DMPOX formation on pH of the media was investigated. Reaction was carried out in 20 mM Tris–HCl solution and adjusting its pH with either HClO_4 or HCl to span the range from 2 to 10 (Fig. 7). In the presence of HClO_4 , DMPOX formation reached a maximum at pH ~ 4 , while this maximum changed to pH 6 in HCl-containing buffer. Also, no DMPOX or any other radical species signals were detected below pH 6 in the solution containing HCl. Since at pH ≤ 5 , a considerable amount of HCl had to be added in order to reach the desired pH, this lack of Tl(III) effect on DMPOX formation suggests a role of Cl^- in this process. This possibility was assessed by carrying out the reaction in a 20 mM Tris–HCl buffer adjusted to pH 4 with HClO_4 , and containing increasing amounts of NaCl (inset to

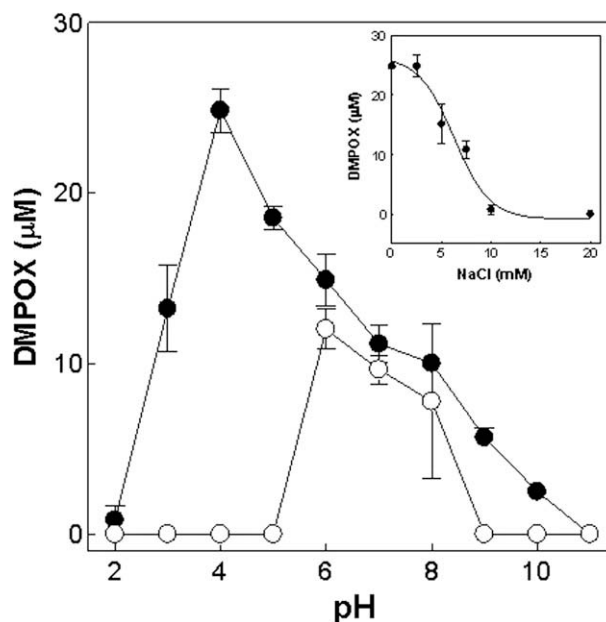


Fig. 7. Effect of pH and Cl^- ion on the reaction between 25 μM Tl(III) and 10 mM DMPO. DMPOX concentration is expressed as a function of media pH given by 20 mM Tris–HCl solutions adjusted to pH 2–10 with HClO_4 (●) or HCl (○). Inset: Amount of DMPOX generated in the presence of variable amounts of Cl^- (2.5–20 mM NaCl).

Fig. 7). DMPOX formation was lower in the presence of the salt, and since Tl(III) is capable to form stable complexes with Cl^- (i.e., TlCl_4^- , $[\text{Tl}_2\text{Cl}_9]^{3-}$), the interaction between the metal and DMPO should be impeded.

At low Cl^- concentrations, DMPOX production efficiency profile depended on Tl(III) apparent charge, given by the number of HO^- moieties included in the hydration sphere of Tl(III). For example, when comparing the distribution of Tl(III) hydroxyl species [30] and Tl(III)-mediated DMPOX formation at the different pH assayed, it is noticeable that the active species is not the free cation itself (Tl^{3+}), but the water-soluble $\text{Tl}(\text{OH})_2^+$ ($\log K_1 = 11.31$) and TlOH_2^+ ($\log K_2 = 7.64$) which predominate within the 3–8 pH range [30]. However, if the initial water addition to DMPO is considered as equilibrium, this reaction would not be favored at low pH, for H_3O^+ being a poor nucleophile. Therefore, the lack of DMPOX formation would not be determined by the absence of a Tl^{3+} -DMPO association but due to the impairment of water addition to the probe. At pH 8, the predominant species is the scarcely soluble $\text{Tl}(\text{OH})_3$ ($\text{pKps} = 45.2$) [30]; given the low solubility of this non-charged species a lower interaction with DMPO is expected. At $\text{pH} \geq 9$, $\text{Tl}(\text{OH})_3$ is redissolved by forming $\text{Tl}(\text{OH})_4^-$. Accordingly with the negative charge of this species, the interaction with DMPO nitrene is not favored, and no evidence of DMPOX formation was observed.

4. Conclusions

This work describes the reaction of the most common nitrones of biological interest with Tl(III). Results demonstrated that Tl(III) in aqueous environment caused the oxidation of DMPO with formation of DMPOX via a free-radical-independent process. Based on the provided evidence, we propose that this reaction proceeds through a Forrester–Hepburn mechanism via the nucleophilic addition of water to produce DMPO-OH, followed by immediate oxidation to DMPOX. The inductive effect of Tl(III) on nucleophilic addition to DMPO was also demonstrated with methoxide in methanol. Kinetic studies showed that Tl(III) disappearance rate was higher (1.6 times) than DMPOX formation rate and equal to Tl(I) formation rate, suggesting a stoichiometry 1.5:1 for Tl(III):DMPOX and 1:1 for Tl(III):Tl(I), in agreement with the proposed mechanism. These conclusions are not extensive to the non-cyclic nitrones POBN and PBN where different mechanisms would be operative and further investigations are necessary to elucidate them. Together, these findings introduce a cautionary note regarding the use of these nitrene compounds in the study of biological samples containing strongly oxidant heavy metals, such as Tl(III).

Acknowledgements

This work was supported by Grants from CONICET (PIP 5536), the University of Buenos Aires (B 072, B 128, B 802) and the Agencia Nacional de Promoción Científica y Tecnológica (PICT 12285), Argentina. S.V., S.L. and M.G. are career investigators from CONICET. Authors are grateful to Dr. Albertina Moglioni for her kind advice.

References

- [1] ATSDR, Thallium, ATSDR (Agency for Toxic Substances and Disease Registry). Prepared by Clement International Corp., under Contract 205-88-0608, Atlanta, GA, 1999.
- [2] R.D. Shannon, *Acta Crystallogr.*, A 32 (1976) 751.
- [3] G. Ma, A. Molla-Abbassi, M. Kritikos, A. Ilyukhin, F. Jalilehvand, V. Kessler, M. Skripkin, M. Sandstrom, J. Glaser, J. Naslund, I. Persson, *Inorg. Chem.* 40 (2001) 6432.
- [4] H. Schwarz, D. Comstock, J. Yandell, R. Dodson, *J. Phys. Chem.* 78 (1974) 488.
- [5] A. Alberti, D. Macciantelli, P. Astolfi, L. Greci, D. Döpp, R. Petrucci, *New J. Chem.* 27 (2003) 1045.
- [6] G.R. Buettner, L.W. Oberley, *Biochem. Biophys. Res. Commun.* 83 (1978) 69.
- [7] H.D. Revanasiddappa, T.N. Kiran Kumar, *Anal. Sci.* 18 (2002) 1131.
- [8] R.A. Floyd, L.M. Soong, *Biochem. Biophys. Res. Commun.* 74 (1977) 79.
- [9] G.M. Rosen, E.J. Rauckman, *Mol. Pharmacol.* 17 (1980) 233.
- [10] W. Chamulitrat, N. Takahashi, R.P. Mason, *J. Biol. Chem.* 264 (1989) 7889.
- [11] C.M. Jones, M.J. Burkitt, *J. Chem. Soc., Perkin Trans. 2* (2002) 2044.
- [12] A. Lawrence, C.M. Jones, P. Wardman, M.J. Burkitt, *J. Biol. Chem.* 278 (2003) 29410.
- [13] P.M. Hanna, W. Chamulitrat, R.P. Mason, *Arch. Biochem. Biophys.* 296 (1992) 640.
- [14] T. Ozawa, Y. Miura, J. Ueda, *Free Radical Biol. Med.* 20 (1996) 837.
- [15] S. Leonard, P.M. Gannett, Y. Rojanasakul, D. Schwegler-Berry, V. Castranova, V. Vallyathan, X. Shi, *J. Inorg. Biochem.* 70 (1998) 239.
- [16] A. Nakajima, Y. Ueda, N. Endoh, K. Tajima, K. Makino, *Can. J. Chem.* 83 (2005) 1178.
- [17] D.P. Barr, R.P. Mason, *J. Biol. Chem.* 270 (1995) 12709.
- [18] J. Van der Zee, *Biochem. J.* 322 (1997) 633.
- [19] A.B. Ross, B.H.J. Bielski, G.V. Buxton, D.E. Cabelli, C.L. Greenstock, W.P. Helman, R.E. Huie, P. Neta, NIST Standard Reference Database 40, NDRL/NIST Solution Kinetic Database, Distributed by National Institute of Standards and Technology (NIST) Standard Reference Data, Gaithersburg, MD, USA, 1992.
- [20] P. Zatta, M. Favarato, M. Nicolini, *Neuroreport* 4 (1993) 1119.
- [21] K. Makino, T. Hagiwara, A. Hagi, M. Nishi, A. Murakami, *Biochem. Biophys. Res. Commun.* 172 (1990) 1073.
- [22] L. Ebersson, *J. Chem. Soc., Perkin Trans. 2* (2) (1994) 171.
- [23] M.L. McCormick, G.R. Buettner, B.E. Britigan, *J. Biol. Chem.* 270 (1995) 29265.
- [24] A. Alberti, P. Carloni, L. Ebersson, L. Greci, P. Stipa, *J. Chem. Soc., Perkin Trans. 2* (1997) 887.
- [25] P. Henry, *J. Am. Chem. Soc.* 88 (1966) 1597.
- [26] A. McKillop, D. Perry, M. Edwards, S. Antus, L. Farkas, M. Nogradi, E. Taylor, *J. Org. Chem.* 41 (1976) 282.
- [27] R. Weast (Ed.), *Handbook of Chemistry and Physics*, 51st ed., The Chemical Rubber Co., Cleveland, Ohio, 1970.
- [28] M.J. Davies, T.F. Slater, *Biochem. J.* 240 (1986) 789.
- [29] F. Chen, Y. Xie, J. He, J. Zhao, *J. Photochem. Photobiol. A: Chem.* 138 (2001) 139.
- [30] T.S. Lin, J. Nriagu, *J. Air Waste Manage. Assoc.* 48 (1998) 151.